Available online at www.sciencedirect.com
SCIENCE DIRECT
Polymer 45 (2004) 8221–8229
polymer
www.elsevier.com/locate/polymer

Nanoindentation and morphological studies on nylon 66/organoclay nanocomposites. II. Effect of strain rate

Lu Shen[a], In Yee Phang[a,1], Tianxi Liu[b,*], Kaiyang Zeng[c]

[a]*Institute of Materials Research and Engineering, 3 Research Link, Singapore, Singapore 117602*
[b]*Institute of Advanced Materials, Fudan University, 220 Handan Road, Shanghai 200433, People's Republic of China*
[c]*Department of Mechanical Engineering, The National University of Singapore, 10 Lower Kent Ridge Crescent, Singapore, Singapore 119260*

Received 11 May 2004; received in revised form 19 July 2004; accepted 1 September 2004
Available online 13 October 2004

Abstract

Strain rate effects on surface deformation behavior of exfoliated nylon 66 (PA66)/organoclay nanocomposites have been explored by nanoindentation in present study. Sharp indenter (Berkovich) has been used to indent on the surfaces of polymer/clay nanocomposite with different strain rates. Significant strain-rate hardening has been found consistently existing in both neat PA66 and its nanocomposite systems from surface to subsurface (a few micron deep into the bulk). However, strain rate shows almost no effect on the elastic moduli of the neat system and the nanocomposites. The elastic modulus and hardness increase with the indentation depth due to inhomogeneous distributions of the crystalline morphology as well as clay concentration for the case of the nanocomposites along the indentation direction. The mechanical properties observed are correlated with the inhomogeneous microstructures of the studied systems. The plastic index of PA66 and the nanocomposites have been evaluated as a function of strain rate.

Keywords: Nylon 66; Nanocomposites; Nanoindentation

1. Introduction

As a new and advanced technique, nanoindentation can provide a wealth of valuable quantitative information regarding the mechanical properties, including elastic, plastic as well as viscoelastic properties of a variety of materials [1,2]. This method relies on the local deformation induced on a material surface with an indenter with specified geometry under the application of a given load. In an indentation experiment, the yield stress is normally exceeded and the indentation depth variation is a combination of both the elastic and plastic contributions to the total indentation depth. One of the main advantages of nanoindentation is that it could probe the mechanical properties of the materials at specified locations on the material surface and measured properties could be quantitatively correlated with the microstructure of the material. By nanoindentation, hardness and elastic modulus can be derived from the load–displacement curve [2], which are closely related to materials physical and mechanical property changes [3]. For example, for polymers, hardness (H) is linearly related to the plastic yield stress (σ_y) with the ratio of H/σ_y approaching 3 for crystalline (plastic) polymers [4,5]. Tabor [6] showed that for metals which are almost entirely plastic in their nature, the ratio of H/σ_y is equal to 3. It is expected that, through hardness measurements, nanoindentation technique could detect the changes of microstructures as well as yield strength of the polymers.

In the past decade, nanoindentation method has been employed extensively to characterize the mechanical properties of various polymeric systems [7–10], such as in polyvinylchloride, poly(ethylene oxide), poly(acrylic acid) [11], poly(ethylene terephthalate) [1,12,13], nylon 6 and their blends or composites [14]. However, less attention is paid to their mechanical properties under different loading conditions [15,16], never mentioned the investigation by

* Corresponding author. Tel.: +86 21 55664197; fax: +86 2165655123.
E-mail address: txliu@fudan.edu.cn (T. Liu).
[1] Current address: Department of Materials Science and Technology of Polymers, Faculty of Science and Technology, University of Twente, P.O. Box 217, 7500 AE ENSCHEDE, The Netherlands.

0032-3861/$ - see front matter © 2004 Elsevier Ltd. All rights reserved.
doi:10.1016/j.polymer.2004.09.062

means of nanoindentation. It is known that the mechanical properties of most materials vary with the rate of loading and this effect is particularly evident in polymers. In general, the mechanical behavior is closely tied to the manner in which the polymer chains move relative to one another under load and the deformation process of polymer chains depends on both time and the rate at which the load is applied [17]. Generally, increasing the strain rate has the effect of increase in yield stress and modulus of a polymer [3,18]. By tensile test, for example, it was reported that the yield stress (and the flow stress of a given strain) of polystyrene (PS) increase significantly with increasing the strain rate, and for nylon 6 and nylon 66 (PA66), their yield stresses can be increased by 5 MPa per decade with increasing strain rate [18]. The sensitivity of modulus to strain rate is most significant in the glass transition region where there is less limitation to the molecular movement. However, this sensitivity is greatly diminished when the temperature is much lower than the glass transition temperature (T_g).

In present study, nanoindentation technique is employed to study the PA66/clay nanocomposites with effect of strain rate. A few studies on the preparation and structures (particularly crystal transition or polymorphism) of PA66/clay nanocomposites have been reported recently [15,16,19–25]. In our previous work [26], the clay concentration (less than 5 wt%) and its distribution in the PA66 matrices are found to greatly affect the thermal as well as mechanical properties of the nanocomposites probably due to the large surface area of the nanoclay platelets and their fine dispersion within the polymeric matrix. In current study, the mechanical behavior including plastic, elastic and viscoelastic properties of PA66 and its nanocomposite are studied under different strain rates by nanoindentation.

2. Theory

2.1. Nanoindentation with continuous stiffness module (CSM)

In conventional indentation test, indenter is driven into the material surface by a static load, and the material stiffness only can be measured from the unloading portion of the experiment [2]. In the CSM technique, an oscillated force is imposed on the indenter while monitoring its response displacement. The characteristic of the material properties, including phase and amplitude of displacement response can be measured. The material stiffness (S) and contact damping (ωC) along indentation loading at the frequency of the oscillation can be calculated using the following Eqs. (1) and (2), respectively. The elastic modulus and hardness are calculated using stiffness data from Eqs. (3) and (4), respectively. Therefore, the hardness and modulus are determined as a function of indentation depth with a single loading/unloading cycle.

$$S = \left[\frac{1}{\frac{P_{max}}{h(\omega)}\cos\Phi - (K_s - m\omega^2)} - K_f^{-1}\right]^{-1} \quad (1)$$

$$\omega C = \frac{P_0}{h(\omega)}\sin\Phi \quad (2)$$

$$\frac{E}{1-\nu^2} = \frac{\sqrt{\pi}}{2}\frac{1}{\sqrt{A_c}}S \quad (3)$$

$$H = \frac{P_{max}}{A_c} \quad (4)$$

where P_{max} and $h(\omega)$ are driving force and the displacement response of the indenter, respectively; Φ is the phase angle between P_{max} and $h(\omega)$; m is mass of the indenter column; K_s is spring constant at the vertical direction; K_f is frame stiffness. m, K_s and K_f are all constant values for specified indentation system. ω is angle speed which equals to $2\pi f$; f is the driven frequency of the AC signal. ν is Poisson's ratio and set to be 0.35 for current analysis [14]. A_c is contact area at the moment material in contact with indenter with load P_{max}.

Comparing with the conventional mode, where the stiffness is determined by analysis of the unloading curve, the CSM technique enables the instrument to determine the contact stiffness throughout the experiment during the loading segment. At each point where a load–displacement data pair is acquired, the viscoelastic or anelastic effects are accounted for [27,28]. In conventional indentation test, the materials, such as polymers, which are strain-rate sensitive materials and prone to room-temperature creep, show widely varying hardness and modulus results depending upon the load–time history for the indentation. Therefore, it is not suitable to derive the mechanical properties of these materials. However, the CSM technique makes it possible to study the polymer's plastic and elastic properties without the effect of maximum holding time and no effect from load–time history is accounted for in the results.

2.2. The strain rate

Strain rate is the imposed rate of deformation during indentation. It is generally correlated with the displacement rate or the loading rate of the indenting body over the softer surface. In an indentation experiment, the strain rate acts nominally in a direction perpendicular to the surface and is defined as the displacement rate ($\dot{h} = dh/dt$) divided by displacement (h) as given by Eq. (5) [7,29].

$$\text{strain rate} = \left(\frac{\dot{h}}{h}\right) \quad (5)$$

2.3. The plasticity index

The plasticity index, ψ, of a solid body is usually used to

characterize the relative plastic/elastic behavior of the material when it undergoes external stresses and strains. In the case of indentation contacts, the area below the loading curve in the load–displacement diagram corresponds to the total energy spent during pressing the indenter into the material. The area below the unloading curve corresponds to the energy released from the system during unloading. Their difference expresses the irrecoverable energy, consisting of the work spent in plastic deformation or other irreversible processes, such as crack, and the elastic energy of residual stresses caused. For the case of polymeric material, one of the definitions for the plasticity index is the ratio of the area encompassed between the loading and unloading curves (equals to plastic work done during the indentation) to the total area encompassed under the loading curve (total work done involves plastic work and viscoelastic recovery). It follows that $\psi = 1$ for a fully plastic deformation, $\psi = 0$ for a fully elastic case, and $0 < \psi < 1$ for viscoelastic–plastic behavior [30].

3. Experimental

3.1. Materials and sample preparation

Neat nylon 66 (PA66) pellets (EPR32, with relative viscosity of 3.2) used in this study were kindly provided by China Shenma Group Co. Ltd Organoclay, Nanomer® I.34TCN (from Nanocor Inc., USA), is a surface modified montmorillonite mineral with a mean particle size of 16–22 μm, which is specifically designed for extrusion compounding and usually used in nylon 6 and nylon 66 systems [31]. PA66 nanocomposites with 5 wt% clay concentration were prepared by melt-compounding using Brabender twin-screw extruder at 280 °C with a screw speed of 180 rpm, followed by pelletizing. The pelletized materials were dried and injection molded into rectangular bars with dimension of $12.5 \times 6.5 \times 160$ mm^3. The detailed studies on preparation, structure/morphology, thermal and mechanical properties of PA66/clay nanocomposites have been reported elsewhere [25]. The specimens were then cut into small pieces suitable to perform nanoindentation tests. After that, the sample surfaces parallel to the injection flow direction were polished using SiC paper in order to remove or eliminate the processing-induced defects or other artifacts until no discernible scratches are observed under optical microscope. After being dried in oven at 60 °C for about 24 h, the polished samples were mounted on aluminum stub using super glue for subsequent indentation tests.

3.2. XRD and DSC measurements

X-ray diffraction (XRD) patterns were recorded using a Bruker GADDS diffractometer equipped with a 2D area detector, operating at a voltage of 40 kV and current of 40 mA using a Cu K_α radiation ($\lambda = 0.15418$ nm). Differential scanning calorimetric (DSC) was performed under nitrogen flow from room temperature to 300 °C at a scanning rate of 10 °C^{-1}min by using a TA MDSC 2900. For both XRD and DSC measurements, three sets of the samples were taken from different locations (i.e. surface, intermediate and core parts) of the injection-molded bulk specimens, and detailed sample preparation is described elsewhere [32]. The weights of samples varied from 4 to 6 mg. The degree of crystallinity was calculated by deconvolution of the XRD patterns. And for comparison, the crystallinity by DSC was estimated by dividing the enthalpies of the samples by the heat of fusion ($\Delta H_m^o = 206$ J g^{-1} [33]) of fully crystalline PA66.

3.3. Nanoindentation experiments

Typical loading–hold–unloading sequence was used to indent on neat PA66 and the nanocomposite with 5 wt% of clay (Fig. 1). Four strain rates, i.e. 2, 5, 10 and 20% s^{-1}, were used to explore the strain rate effect on the mechanical properties of the materials. The typical nanoindentation tests were carried out as follows. After the indenter was

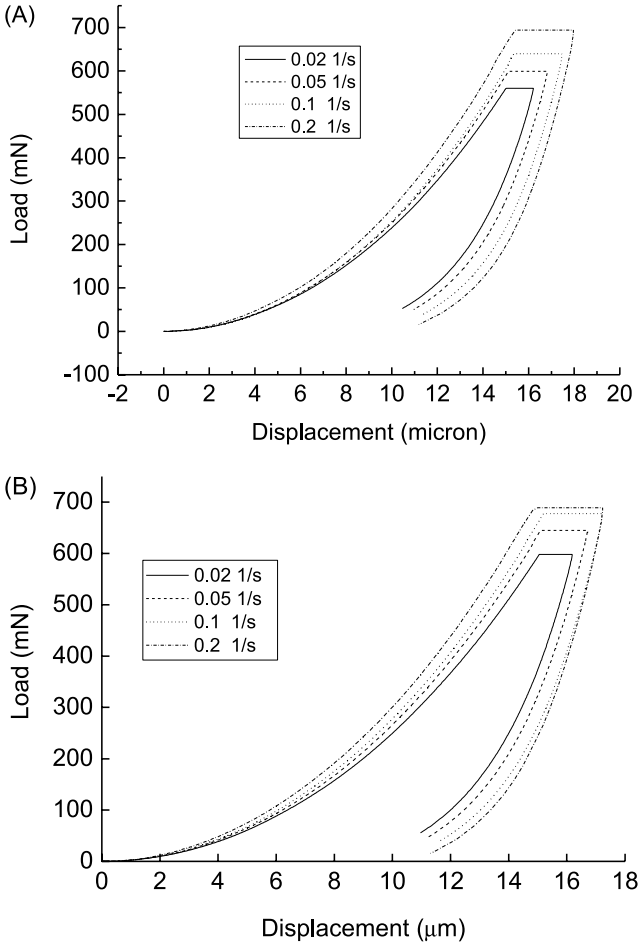

Fig. 1. Loading–hold–unloading curves showing strain rate effect for neat PA66 (A) and its nanocomposite containing 5 wt% clay (B).

successfully in contact with the surface, it approached into the material with pre-defined strain rate until 15 μm deep into the surface; the load was then held at the maximum value for 60 s in order to minimize the creep effect on unloading session; and finally, the indenter was withdrawn from the surface with the same rate as loading process until the load decreasing to 10% of the maximum load. Another series of test was carried out on the same material with maximum depth to be 10 μm and without holding time at maximum load. The purpose of the latter test was to evaluate the plasticity index of the polymer where no plastic displacement contribution from the material creep (i.e. hold segment) is considered. At least 10 indents were performed on the polished sample surfaces. One hundred micrometer was chosen as interval between each two indents to avoid interaction.

A three-side pyramid (Berkovich) diamond indenter was employed for the indentation experiments. The area function, which is used to calculate contact area A_c from contact depth h_c, was carefully calibrated by using standard sample, fused silica, prior to the experiments.

4. Results and discussion

4.1. Effect of strain rate on load–displacement curves

Fig. 1(A) and (B) are typical loading–hold–unloading curves with different strain rates for neat PA66 and its nanocomposite with 5 wt% clay, respectively. On loading, the curves steadily shift upwards with increasing the strain rate, indicating that the resistance of the materials to indentation gradually increases with strain rate. The maximum loads at the hold segments are tabulated in Table 1. For both neat and composite systems, the maximum load increases steadily with strain rate. The overall loads at different strain rates for the nanocomposite are higher than those for neat system as addition of stiff clay increases the material's resistance to indentation. However, the difference between the two systems at lower strain rates (0.02–0.1 s^{-1}) is more prominent than that at higher strain rate (0.2 s^{-1}). It seems that with high strain rate, it is relatively difficult to discover the effects of clay addition on the materials' resistance to indentation. This phenomenon is related to the plastic index of the material as to be discussed later.

Table 1
Strain rate effect on the maximum loads of neat PA66 and its nanocomposite with 5 wt% clay

Strain rate (s^{-1})	Maximum load at indentation depth of 15 μm (mN)	
	Neat PA66	PA66/clay (95/5)
0.02	561.8±8.2	597.3±1.5
0.05	594.3±13.2	641.0±4.6
0.1	632.4±6.9	662.8±3.7
0.2	686.1±7.9	681.0±8.6

The loading curves are followed by a period of holding time (here, 60 s) at which the peak loads are kept constant to permit the material under load to relax before unloading. During unloading, the load is reduced at the same rate as in the loading cycle. In this case, the elastic displacements are recovered. It can be seen that significant creep was clearly found in the maximum hold segments for both neat PA66 and the nanocomposites. In particular, the (creep) depths or displacements significantly increase with increasing strain rate, suggesting that increasing strain rate on loading segment leads to greater creep susceptibility of the materials.

4.2. Effect of strain rate on hardness

Fig. 2(A) and (B) illustrate the hardness profiles for neat PA66 and its nanocomposite with 5 wt% clay, respectively. For neat PA66 (Fig. 2(A)), the hardness generally increases with increasing the strain rate, indicating that significant increase in yield stress has occurred. The hardness value (averaged in the range of 4–5 μm) increases by about 21%

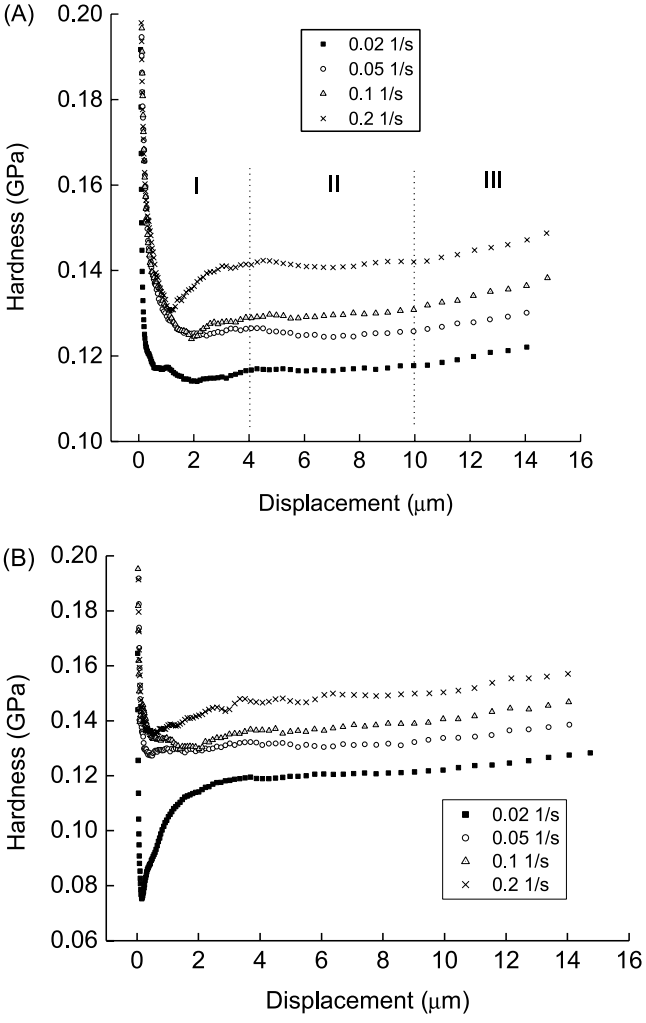

Fig. 2. Effect of strain rate on the hardness of PA66 (A) and the nanocomposite containing 5 wt% clay (B).

from 111 to 134 MPa when increasing one order of strain rate (from 0.02 to 0.2 s^{-1}). Table 2(a) lists the hardness and modulus calculated by CSM method with four different strain rates. For neat PA6 and PA66, it was reported that the increment of yield stress by tensile test is only about 5 MPa when increasing strain rate per decade [18]. It shows that, therefore, with nanoindentation technique where the material deforms in compression mode, the degree of improvement in yield stress with increasing strain rate is greatly larger than the effect observed in the tensile test. A possible reason causing the difference between the two measurements (i.e. tensile and indentation) is the loading direction for the tensile test is along the injection flow direction; while in an indentation test, loading direction is perpendicular to the flow direction. The relative orientation of polymer chains and clay platelets (induced by polymer processing) to loading direction may have effect(s) on the mechanical properties of the injection-molded specimen, thus leading to the discrepancy in the materials' response to the external load in two perpendicular directions.

For neat PA66 system, with a given strain rate, the hardness profile could be generally divided into three regions, as shown in Fig. 2(A). In region I, i.e. from surface to approximate 4 μm, the hardness dramatically decreases followed by a slight increase with increasing the indentation depth. The initial decrease of the hardness may be due to the indentation size effect or some uncertainties existing at the very surface layer of the material [34]. After that, the slight increase of the hardness with the indentation depth (displacement) is probably due to the inhomogeneous distribution of crystalline morphology (e.g. crystallinity) in the injection-molded specimens along the indentation direction [25]. Generally, due to the effect of temperature gradient, the outer skin part of a molded bar experiences an air-quenching process (i.e. less or even no time to crystallize) upon injection molding, as evidenced below by XRD and DSC. In this region, amorphous population is dominant, while the degree of crystallinity slightly increases along the indentation direction (into the bulk), which may cause slight increment of the hardness. In region II, i.e. from about 4–10 μm, the hardness of neat PA66 roughly stabilizes at certain values. This region may be considered as a 'transition zone', which illustrates the microstructural changes from the amorphous 'skin' to crystalline 'core' in the injection-molded specimens. In region III, i.e. from 10 μm onwards, the hardness again shows to increase steadily with indentation displacement. It is believed that the inner (or 'core') part undergoes a slow/long cooling process (i.e. having much time to crystallize), thus having higher degree of crystallinity than the outer portion, and consequently leading to increment of the hardness with indentation depth.

Table 2(a)
Modulus and hardness calculated from CSM method (averaged in the depth range of 4–5 μm) of neat PA66 and its nanocomposites

Strain rate (s^{-1})	Modulus (GPa)	Hardness (GPa)
Neat PA66		
2	2.54±0.04	0.117±0.004
5	2.52±0.06	0.126±0.008
10	2.49±0.07	0.129±0.005
20	2.48±0.05	0.142±0.007
PA66/Clay (99/5)		
2	2.67±0.05	0.119±0.004
5	2.70±0.03	0.132±0.003
10	2.66±0.034	0.136±0.002
20	2.69±0.09	0.147±0.005

Table 2(b)
Modulus and hardness calculated from unloading slope *without maximum hold segment* (Oliver–Pharr method) of neat PA66 and its nanocomposites

Strain rate (s^{-1})	Modulus (GPa)	Hardness (GPa)
Neat PA66		
2	2.06±0.04	0.122±0.003
5	2.07±0.03	0.125±0.003
10	2.10±0.03	0.128±0.003
20	2.06±0.08	0.134±0.002
PA66/Clay (99/5)		
2	2.26±0.04	0.126±0.002
5	2.27±0.04	0.126±0.002
10	2.35±0.08	0.134±0.002
20	2.35±0.54	0.139±0.004

The above-mentioned microstructural variations from surface to core regions of the injection-molded specimens were confirmed by XRD and DSC studies. The XRD patterns of different locations (i.e. surface, intermediate and core parts) of the injection-molded neat PA66 bulk specimens are shown in Fig. 3. The degree of crystallinity was calculated by deconvolution of the XRD patterns and tabulated in Table 3. It can be seen that the crystallinity by XRD ($W_{c,x}$) increases from outer or skin layer to the central

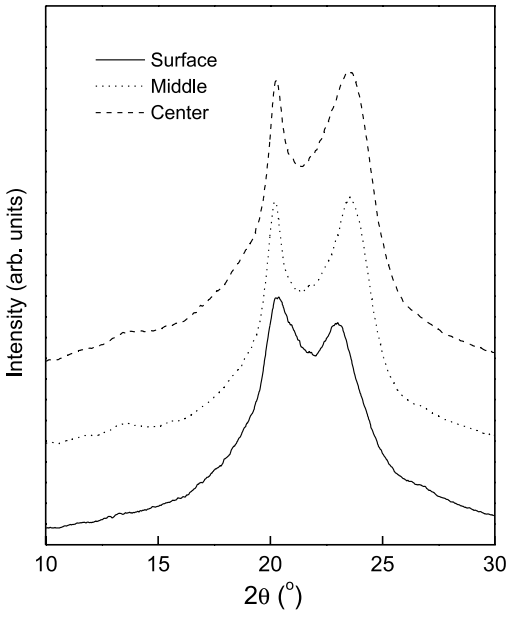

Fig. 3. XRD patterns of different regions (i.e. surface, intermediate, and core) of injection-molded specimens for neat nylon 66.

or core region of the molded specimen. This is mainly due to the effect of thermal gradient upon injection molding. Similar results have been reported recently for nylon 6 and its clay nanocomposites by Paul and co-workers [35] and Cakmak and co-workers [36]. The crystallinity estimated by DSC ($W_{c,h}$) was also included in Table 3(a) and (b) for comparison, showing that the crystallinities by XRD and DSC have the same changing tendency but with different values, that is, $W_{c,h} > W_{c,x}$. This is probably because some (amorphous or less ordered) material usually undergoes reorganization during heating process in DSC, and the reorganized population may contribute to the melting event.

It shows slightly different behavior for the case of the nanocomposite with 5 wt% clay, where the hardness profiles gradually increase with increasing penetration depth after approximately 1 μm into the polymer surface (Fig. 2(B)). The three regions observed for neat PA66 become unclear for the nanocomposite system. That is, the existence of clay has blurred the microstructural changes from the amorphous-dominated to the crystalline-dominated regions along the indentation direction. Besides the temperature gradient effect discussed above in neat PA66, clay addition is also responsible for the gradual increase of the hardness with increasing indentation depth. It has been found that, for nylon 6/clay nanocomposites [32], a gradient distribution of nanoclay induced by injection-molding was clearly evidenced by optical microscopy, X-ray diffraction and thermal analysis. That is, clay concentration gradually increases from the surface to the inner part for the molded bulk (tensile or bending) bars. This flow-induced pattern for clay distribution is usually formed and often observed during polymer melt processing. Therefore, the increase of hardness with indentation depth for the nanocomposites is probably due to not only a temperature gradient effect but also an inhomogeneous clay distribution from the surface to the core of the molded specimens. The microstructures (consequently the mechanical properties) of the matrix are substantially affected by the two factors.

Similar to the neat system, PA66/clay nanocomposite clearly shows that the hardness increases with increasing the strain rate (Fig. 2(B)). The increment gradient of hardness, due to inhomogeneous dispersion of clay and gradient distribution of crystallinity, is almost the same for each individual hardness profile for a given strain rate. As shown in Table 2(a), the hardness values, which are averaged in the range of 4–5 μm, increase by about 23% from 120 to 147 MPa for increasing one order in strain rate. The data show that, except that the clay loading increases the overall hardness of the nanocomposites, the strain-rate hardening effect is similar for neat system and the nanocomposites. This probably indicates that the exfoliated clay platelets do not affect strain rate sensitivity of the matrix. At very low strain rate (e.g. 0.02 s^{-1}), the hardness behavior at shallow depth, i.e. less than 1 μm, shows to be somehow unusual behavior where an abrupt decrease followed by a sudden increase of the hardness is observed for the nanocomposite. Again, this may be due to the indentation size effect or the uncertainties existing in the very surface area (less than 1 μm) and detailed studies in this area are worth to be done in the future.

Table 3
Crystallinity data from XRD patterns (after theoretical fitting) and DSC curves obtained on different regions (i.e. surface, intermediate, and core) of injection-molded specimens for neat nylon 66

	Surface	Intermediate	Core
Crystallinity by XRD, $W_{c,x}$ (%)	29	33	37
Crystallinity by DSC, $W_{c,h}$ (%)	37	45	48

4.3. Effect of strain rate on elastic modulus

Elastic modulus profiles for neat PA66 and its nanocomposite with 5 wt% clay are shown in Fig. 4(A) and (B), respectively. Different from the hardness profiles, the strain rate has insignificant effect on elastic modulus profiles. This phenomenon agrees very well with the findings by Harold

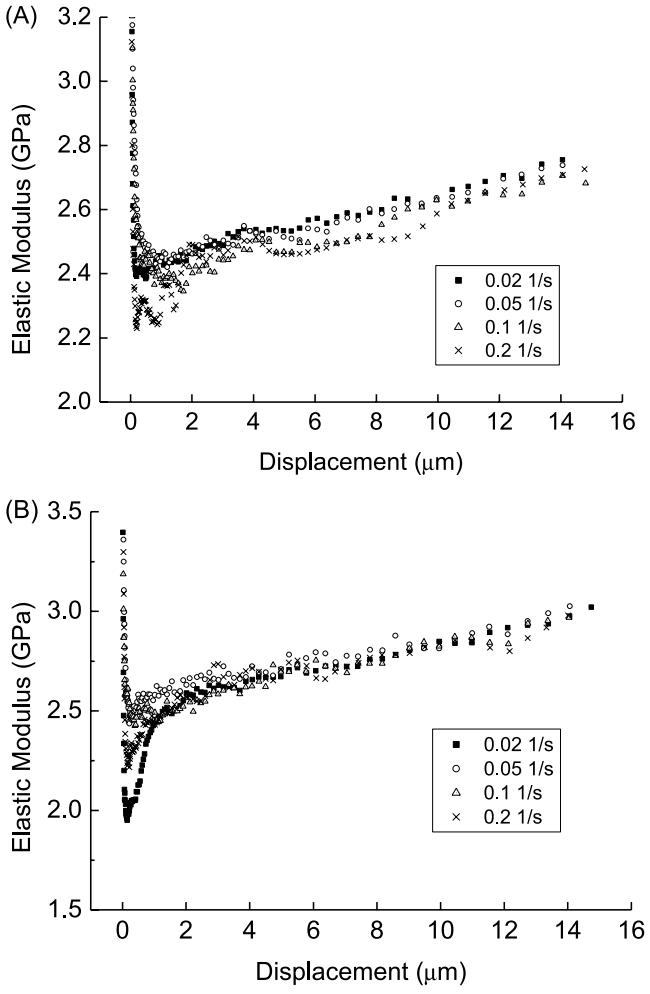

Fig. 4. Effect of strain rate on the elastic moduli of neat PA66 (A) and its nanocomposite containing 5 wt% clay (B).

[18] where the strain rate only has effects on plastic and viscoelastic properties of PS but has slight effect on elastic modulus of the polymer. The elastic constants (such as elastic modulus, shear modulus and Poisson's ratio), which are in principle sensitive to strain rate, are mainly determined by the amorphous fraction in the semicrystalline materials [3]. When temperature is much lower than T_g, the thermal energy available falls below the energy required for chain segments thus overcoming the potential barriers to movement. The system is therefore 'locked' into a glassy state. In this state, the sensitivity of the elastic modulus to strain rate effect becomes less with decreasing temperature. Lower than half of the T_g, the effect of strain rate on the elastic properties of the amorphous polymer is reported to be nearly nil [3]. For PA66, its T_g is about 50 °C [25], which is higher than the room temperature where the indentation tests are performed. This probably gives the possible explanation of the insensitivity of modulus to the strain rate changes in indentation study. Thus, it may come to the conclusion that the increased resistance to indentation with higher strain rate, as shown in Fig. 1, is mainly attributed to the increased yield stress with increasing strain rate.

To verify the conclusion drawn on the hardness–strain rate sensitivity, Oliver and Pharr (O–P) analysis [2] has been employed to calculate the hardness and modulus responses to strain rate. To exclude the viscoelastic/anelastic effect on unloading slope, no maximum hold is applied in the indentation test. The calculated values of hardness and modulus are listed in Table 2(b). The calculation on the indentation tests without maximum holding segments (Fig. 6) by O–P method shows that the hardness for the neat system increases steadily from 0.122 GPa at 0.02 s^{-1}, to 0.134 GPa at 0.2 s^{-1}. For the case of the nanocomposite with 5 wt% clay, the hardness increases from 0.126 GPa at 0.02 s^{-1}, to 0.139 GPa at 0.2 s^{-1}. In both cases, the hardness increases by approximately 10%, while there is insignificant change in the modulus, indicating that the calculations from O–P (Table 2(b)) and CSM (as shown in Table 2(a)) methods give similar trend on the strain-rate sensitivity for the studied systems.

It is also noted that the modulus values for all the samples steadily increase with indentation depth from 1 to 5 μm, especially for the nanocomposite. For neat system, however, there is almost no effect resulting from the distribution of nanoclay platelets within the matrix as explained previously. It is well known that the elastic modulus of polymer greatly depends on the degree of crystallinity [37]. Obviously, for the PA66/clay nanocomposite, the inhomogeneous distributions of both clay and crystallinity function simultaneously which lead to much faster increment of the modulus with increasing the indentation depth. In order to confirm the above speculations, i.e. the inhomogeneous microstructure resulting from the temperature gradient effect in injection-molded parts, similar indentation experiment was performed on a highly crystallized neat PA66 specimen (which was annealed at 200 °C in an oven for 24 h). The purpose of this annealing process is to diminish the inhomogeneous distribution of crystallinity from the surface to the inner part of the molded specimen. Fig. 5 illustrates the hardness and the modulus profiles of the highly crystalline PA66 sample. Compared with the results shown in Figs. 2(A) and 4(A) for the as-molded samples of neat PA66, it can be clearly seen that from the very first surface (approximately 200 nm onwards), both hardness and modulus are almost stabilized at certain *constant* values, i.e. 0.19 and 3.29 GPa for the hardness and the modulus, respectively, with increasing the penetration depth. It indicates that long time annealing greatly diminishes the microstructural inhomogenity from the sample surface to the bulk, which is originated from the temperature gradient effect upon injection molding. And, the hardness and the modulus of the annealed sample are much higher than those (0.12 and 2.5 GPa, respectively) of the as-molded one, due to high degree of crystallinity after annealing.

4.4. Effect of strain rate on plasticity index

The loading–unloading curves at different strain rates are shown in Fig. 6(A) and (B) for PA66 and its nanocomposite, respectively. The data presented here are evaluated without plastic displacement contribution of the material creep (i.e. the maximum hold segments). Generally, the materials appear more plastic in nature under higher strain rate. This phenomenon is explained as follows: with fast strain rate, there is less time for the polymer chains in amorphous population to recover elastically after the external load removes, thus leading to plastic deformation left in the material. Fig. 6(C) shows the plasticity index (ψ) under different strain rates for neat PA66 and its nanocomposite. It is also noticed that, at higher strain rate (0.2 s^{-1}), the plastic indices for the two systems have similar values. It indicates that, the materials behave more plastically with fast loading rate, even for a ductile material like neat PA66. The effect of

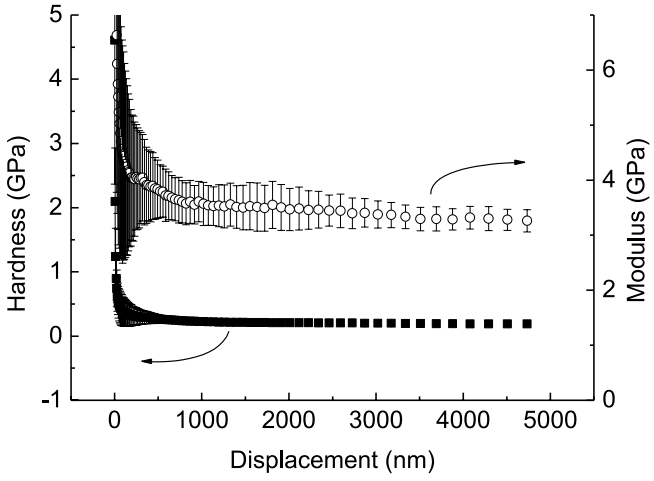

Fig. 5. Hardness and elastic modulus of neat PA66 annealed at 200 °C under vacuum for 24 h.

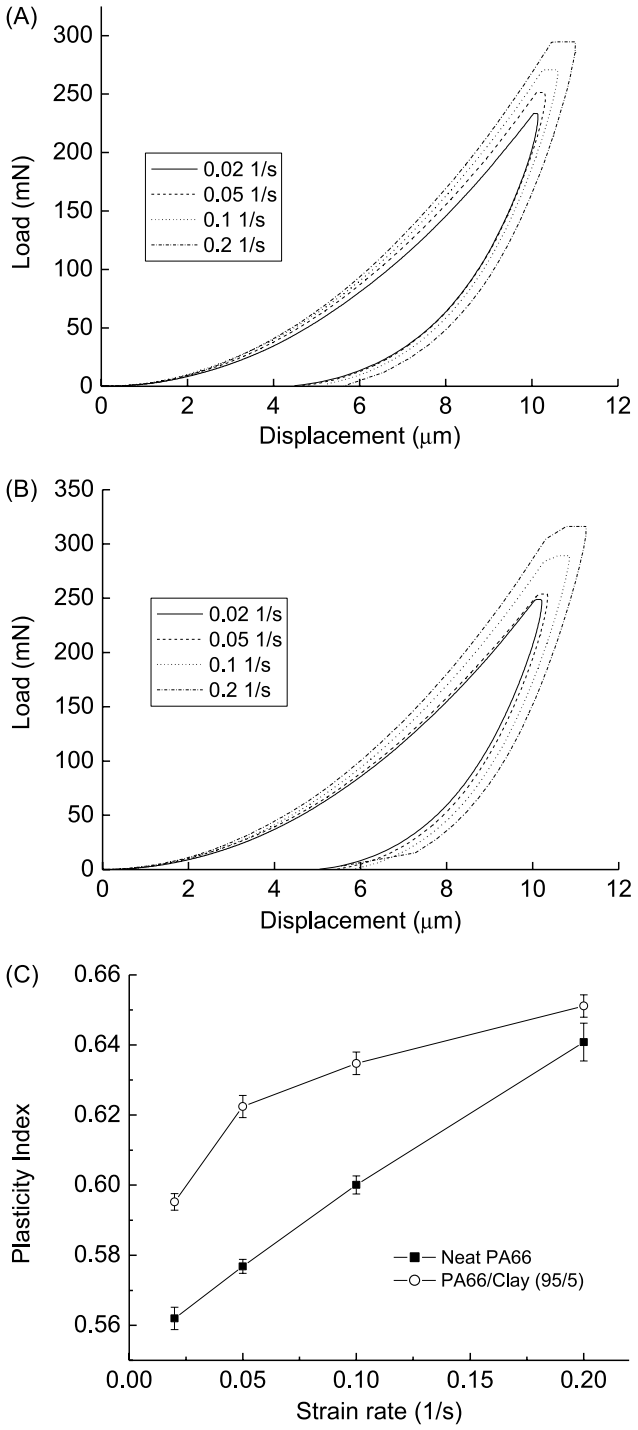

Fig. 6. Loading–unloading curves for PA66 (A) and its nanocomposite containing 5 wt% clay (B), and their plasticity index as a function of strain rate (C).

clay addition in the nanocomposite is less prominent under this condition.

Clearly, the overall values of ψ at different strain rates for the nanocomposite are higher than those of the neat system. This indicates that the addition of stiff clay platelets could restrict the elastic recovery of the deformed molecules of the polymer matrix when the external load has been removed. It may explain why the PA66/clay nanocomposites are much less ductile and more brittle than the neat system [31].

5. Conclusions

Nanoindentation has been proven to be a suitable and valuable technique which can provide localized mechanical properties of the polymer and its nanocomposites. In present study, the effects of strain rates on the plastic (hardness), elastic (modulus) and viscoelastic (creep) behavior of PA66 and its nanocomposites have been comparatively investigated by nanoindentation. And, the mechanical properties observed have been correlated with the microstructures of the materials used. Pronounced strain-rate hardening effect has been observed for both neat PA66 and the nanocomposite samples. Clay addition, however, does not significantly affect the plastic response of the matrix when changing the strain rate. The plasticity index of the neat system and its nanocomposite are shown to increase with the strain rate. The elastic responses of the neat and nanocomposite systems are shown to be insensitive to the strain rate as the motion of the amorphous population in the semicrystalline materials has been 'locked' at the temperature much lower than T_g. The increment of modulus and the hardness with the indentation depth for neat system is due to the inhomogeneous microstructure (e.g. crystallinity) caused by injection molding, namely temperature gradient effect. For the case of the nanocomposites, besides the microstructural changes, the inhomogeneous clay distribution induced by polymer processing is also responsible for the increases of the modulus and the hardness with the indentation depth. The creep susceptibility of both systems is enhanced with strain rate increasing. The studies of the effects of other experimental parameters for nanoindentation (such as holding time, frequency imposed on loading, and so on) on the mechanical properties of PA66/clay nanocomposites are still in progress.

References

[1] Flores A, Balta Calleja FJ. Phil Mag A 1998;78:1283–97.
[2] Oliver WC, Pharr GM. J Mater Res 1992;7:1564.
[3] Swallowe BY. Mechanical properties and testing of polymers. Dordrecht: Kluwer Academic Publishers; 1999.
[4] Sebastia KS. PhD Thesis. Department of Chemical Engineering and Chemical Technology. Imperial College, London, UK; 1994.
[5] Lorenzo V, Perena JM, Faton TG. J Mater Sci Lett 1989;8:1455–7.
[6] Tabor D. The hardness of metals. Oxford: The Clarendon Press; 1951.
[7] Briscoe BJ, Fiori L, Pelillo E. J Phys D Appl Phys 1998;31:2395–405.
[8] VanLandingham MR, Villarrubia JS, Guthrie WF, Meyers GF. Macromol Symp 2001;167:15–43.
[9] Penumadu D, Dutta A, Pharr GM, Files B. J Mater Res 2003;18:1849–53.
[10] Beake BD, Chen S, Hull JB, Gao F. J Nanosci Nanotech 2002;2:73–9.

[11] Nowicki M, Richter A, Wolf B, Kaczmarek H. Polymer 2003;44:6599–606.
[12] Beake BD, Leggett GJ. Polymer 2002;43:319–27.
[13] Flores A, Balta Calleja FJ, Asano T. J Appl Phys 2001;90:6006–10.
[14] Krumova M, Flores A, Balta Calleja FJ, Fakirov S. Colloid Polym Sci 2002;280:591–8.
[15] Liu XH, Wu QJ. Macromol Mater Eng 2002;287:180–6.
[16] Han B, Ji GD, Wu SS, Shen J. Eur Polym J 2003;39:1641–6.
[17] Askeland DR. The science and engineering of materials. London: Chapman & Hall Press; 1996.
[18] Harold GH, van Melick. PhD Thesis. Cip-data Library Technische Universiteit; 2002.
[19] Wu TM, Wu JY. J Macromol Sci Phys 2002;B41:17–31.
[20] Zhu CS, Kang X, He SQ, Wang LY, Lu LY. Chin J Polym Sci 2002;20:551–7.
[21] Liu XH, Wu QJ, Berglund LA. Polymer 2002;43:4967–72.
[22] Yu ZZ, Yang MS, Zhang QX, Zhao CG, Mai YW. J Polym Sci Polym Phys 2003;41:1234–43.
[23] Liu XH, Wu QJ, Zhang QX, Mo ZS. J Polym Sci Polym Phys 2003;41:63–7.
[24] Lu YL, Zhang GB, Feng M, Zhang Y, Yang MS, Shen DY. J Polym Sci Polym Phys 2003;41:2313–21.
[25] Phang IY, Chen L, Tjiu WC, Pisharath S, Liu TX. Mater Res Innovations 2004;8(3).
[26] Shen L, Phang IY, Chen L, Liu TX, Zeng KY. Polymer 2004;45:3341–9.
[27] Lucas BN, Oliver WC, Swindeman JE. Mater Res Soc Symp Proc 1998;522:3–14.
[28] Technical report from MTS Systems Corporation. Expanding the range of measurable properties by indentation experimentation: The nano Indenter® II's continuous stiffness measurement (CSM) option (http://www.mts.com/nano/CSM_mech.htm).
[29] Grau P, Meinhard H, Mosch S. Mater Res Soc Symp Proc 1998;522:153–8.
[30] Johnson KL. Contact mechanics. Cambridge: Cambridge University Press; 1985.
[31] Technical data from Nanocor, Inc. (http://www.nanocor.com).
[32] Liu TX, Tjiu WC, He CB, Na SS, Chung TS. Polym Int 2004;53:392–9.
[33] Sperling LH. Introduction to polymer science. New York: Wiley; 2001.
[34] Nix WD, Gao H. J Mech Phys Solids 1998;46:411–25.
[35] Fornes TD, Paul DR. Polymer 2003;44:3945–61.
[36] Yalcin B, Cakmak M. Polymer 2004;45:2691–710.
[37] Peterlin A. Colloid Polym Sci 1987;265:357.